Ultrasonic enhancement of bead-based bioaffinity assays

M. Wiklund* and H. M. Hertz

Received 22nd November 2005, Accepted 3rd July 2006
First published as an Advance Article on the web 8th August 2006
DOI: 10.1039/b609184a

Ultrasonic radiation forces can be used for non-intrusive manipulation and concentration of suspended micrometer-sized particles. For bioanalytical purposes, standing-wave ultrasound has long been used for rapid immuno-agglutination of functionalized latex beads. More recently, detection methods based on laser-scanning fluorometry and single-step homogeneous bead-based assays show promise for fast, easy and sensitive biochemical analysis. If such methods are combined with ultrasonic enhancement, detection limits in the femtomolar region are feasible. In this paper, we review the development of standing-wave ultrasonic manipulation for bioanalysis, with special emphasis on miniaturization and ultrasensitive bead-based immunoassays.

Introduction

Immunoassay-based techniques for identification and quantification of proteins or other biomolecules are of great importance in biomedical and biochemical analysis, *e.g.*, in clinical diagnostics, in drug discovery/proteomics research, and in food-industry quality controls. In particular, there is a growing demand for sensitive, selective, simple, easy-operational and cost-effective assays that can be easily implemented at clinics and laboratories for routine diagnosis. Here, important factors are reduction in consumption of biochemical reagents and simplification of the assay protocols. Therefore, assay development is moving towards miniaturization, parallelization and the separation-free format. An interesting alternative to standard methods is to employ functionalized beads and external force fields for bead manipulation. Here, we review ultrasonic enhancement in bead-based assays and the potential for such techniques in miniaturized systems.

Today, assays based on nanometer or micrometer-sized beads are often employed, either as solid support or as labels.[1] Beads are advantageous to use in immunoassays for several reasons.[2,3] In comparison to planar surface-binding assays, beads allow much higher binding area per unit volume. This results in high local concentration of the analyte on the beads, which could be several orders of magnitude higher than the concentration of analyte in the total reaction volume.[4] Furthermore, the mobility of suspended beads increases the speed of the assay and allows for flexible scaling of reagent. For example, if the binding capacity of the beads is known, the bead concentration can be optimized for each assay condition, *e.g.*, for the analyte concentration and for the affinity of the assay. Beads are also perfectly suitable for use in miniaturized systems such as chip-based assays.[2] An important factor for the increasing popularity of bead-based assays is the commercial availability of beads. Today, beads may be purchased in different sizes from a few nanometers to hundreds of micrometers, in different materials, with different surface properties, dyed with fluorophores, chemiluminescent molecules or photosensitizers, dyed with combinations of several fluorophores or with various amounts of a single fluorophore, with light-transmitting, electrical or magnetic properties, and coated with a large variety of different biomolecules.[1,3,5] Together with new beads, new assays are developed. An example is suspension array technology (SAT), where multiplexing in a single sample is possible by the simultaneous use of several subpopulations of encoded beads coated with different molecules.[6] However, most important for the context of this paper is the possibility of enhancing a bead-based assay by the use of field-assisted manipulation.[7] In contrast to assays with planar binding surfaces, *e.g.* ELISA-type assays on slides or small spots (microarrays),[8,9] beads can be concentrated, separated and trapped by the use of external force fields. Examples of different techniques for contactless manipulation of microparticles that have been implemented in microsystems are optical,[10] magnetic,[11] dielectrophoretic[12] and acoustic[13] manipulation.

This review will focus on ultrasonic standing-wave (USW) manipulation systems used in bead-based immunoassays. USW manipulation is a powerful tool for large-scale manipulation of suspended microparticles, and can be used for enhancement of bead-based assays.[14] Here, the term large-scale refers to the possibility of performing simultaneous manipulation of all particles in a suspension, in contrast to single-point manipulation methods like optical tweezers[10] and dielectrophoresis.[12] Still, the assay format can be miniaturized in terms of small sample volumes ($\sim\mu$l), and applied to microsystems (*e.g.*, microfluidic chips and microtiter plates). Three different reported approaches to ultrasonic enhancement in bead-based assays exist. The first approach employs the immuno-agglutination assay format, where antibody-coated beads form aggregates in the presence of the antigen (the analyte), see Fig. 1a. Here, USW technology has been used to enhance the bead collision rate for increased speed and sensitivity.[15] The second approach is based on the very initial stage of immuno-agglutination, where two beads form a pair

Biomedical and X-Ray Physics, Royal Institute of Technology, SE-106 91, Stockholm, Sweden. E-mail: martin@biox.kth.se

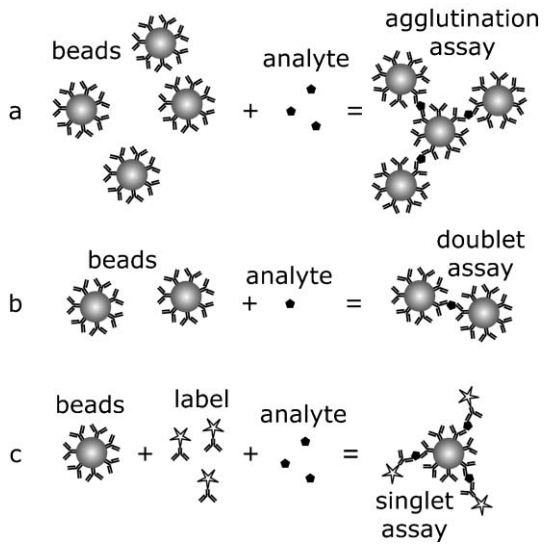

Fig. 1 (a): The bead-based agglutination assay. Beads with capture antibodies are mixed with the analyte, resulting in a bead aggregate. (b): The bead-based doublet assay. The initial stage of agglutination. (c): The bead-based singlet assay. Beads with capture antibodies are mixed with labeled tracer antibodies and the analyte, resulting in sandwich assays on single beads.

(the doublet assay), see Fig. 1b. Here, USW has been used to separate and enrich doublets from single beads in microfluidic capillaries.[16] The last approach is to employ bead-immobilized capture antibodies and fluorophore-labeled tracer antibodies, and sandwich the analyte between the capture and tracer antibodies on single beads (the singlet assay), see Fig. 1c. In this assay, USW technology has been used for enrichment and positioning of bead-immobilized receptors in microtiter plates or microfluidic chips, followed by fluorescence detection.[17,18] The latter method shows promise for ultrasensitive detection with sensitivity in the femtomolar range. In this paper, we evaluate the performance and sensitivity of USW-enhanced bead-based assays in comparison to other available ultrasensitive assays.

Principles and theory of USW manipulation

It has been known since the 19th century that an object in a sound field is affected by a steady-state acoustic radiation force. In a classical experiment, Kundt and Lehman trapped dust particles in a tube by applying a standing-wave field.[19] The dust particles were collected in several lateral lines along the tube, each separated by a distance corresponding to half the wavelength of the sound wave. However, it is only in the last decades the phenomenon has found widespread application.[20–23] More recently, the technology has been successfully implemented in miniaturized systems, such as microfluidic chips,[13,24–32] microfluidic capillaries[16] and microtiter plates[17] (see Fig. 2a–c).

The acoustic radiation force is a result of a non-linear effect in the time-averaged radiation pressure around an object in a sound wave, also known as the time-averaged acoustic Bernoulli pressure. The theoretical treatment below follows the formalism of Gor'kov,[33] who derived a very useful potential

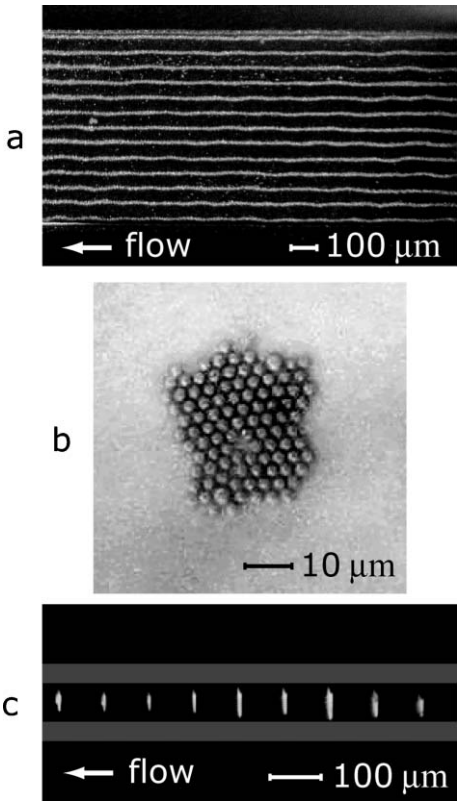

Fig. 2 (a): Multiplexed alignment of 2 μm beads in a silicon microchip with USW field perpendicular to the flow, ~12 MHz frequency. Image adapted from ref. 32. (b): Single-layer, two-dimensional aggregation of 3 μm beads in a microtiter plate, ~3 MHz frequency. Image adapted from ref. 17. (c): Trapping, enrichment and size-selection of 4 μm beads in a microfluidic capillary, ~8 MHz frequency. The capillary walls are marked in gray with correct scale. Image adapted from ref. 16.

function, U, for the time-averaged radiation force on a spherical object with radius r, in an arbitrary shaped standing-wave field:

$$U = V\left(f_1 E_{\text{pot}} - \frac{3}{2} f_2 E_{\text{kin}}\right), \tag{1}$$

where V is the volume of the sphere ($4\pi r^3/3$), and E_{pot} and E_{kin} are the time-averaged potential and kinetic energy densities, respectively, given by

$$\begin{aligned} E_{\text{pot}} &= \frac{\langle p^2 \rangle}{2\rho_0 c_0^2} \\ E_{\text{kin}} &= \frac{\rho_0 \langle v^2 \rangle}{2}. \end{aligned} \tag{2}$$

Here, $\langle p^2 \rangle$ and $\langle v^2 \rangle$ are the mean-square fluctuations of the incident pressure and velocity† of the acoustic field at the point where the object is located, and ρ_0 and c_0 are the density and the sound (phase) velocity‡ of the medium. The factors f_1 and

† The velocity, v, of the acoustic field refers to the velocity of an oscillating volume element of the medium hosting the acoustic wave, and should not be mistaken for the phase velocity, c, of the sound field.
‡ The phase velocity, c, is most often called the sound velocity.

f_2 are dimensionless corrections taking the compressibility of the object into account, and are given by

$$f_1 = 1 - \frac{\rho_0 c_0^2}{\rho c^2}, \quad f_2 = \frac{2(\rho - \rho_0)}{2\rho + \rho_0}, \tag{3}$$

where ρ and c are the density and the sound velocity of the sphere. In the case of a rigid sphere, $f_1 = f_2 = 1$. Eqn (1) is valid under certain conditions for the size of the sphere, namely

$$r \ll \lambda, \; r \gg s_0 \tag{4}$$

where λ is the acoustic wavelength in the medium and s_0 is the medium volume element displacement amplitude.

If the acoustic field geometry is known, the acoustic radiation force on a spherical object is obtained from the potential function by the expression

$$\boldsymbol{F} = -\nabla U \tag{5}$$

Thus, the force on a spherical object is given by the (negative) gradient of the potential function U. A stable trapping point is localized in positions of local minima of the potential function U, satisfying $\boldsymbol{F} = 0$. If only axial forces are considered and assuming a harmonic sound source, the force, $\boldsymbol{F} = F(z)$, is given by

$$F(z) = -\frac{\partial}{\partial z} U(z) = \frac{\pi}{2\rho_0 c_0^3} \left(f_1 + \frac{3}{2} f_2 \right) V p_0^2 v \sin\left(2\pi \frac{z}{\lambda/2} \right). \tag{6}$$

The expression shows that the radiation force varies spatially with the period $\lambda/2$, and that the force is proportional to the volume of the sphere (V), the intensity I of the sound wave (*via* $I = p_0^2/2\rho_0 c_0$), and the frequency v of the sound wave. A typical value of the radiation force acting on a latex bead suspended in water is, *e.g.*, maximum 30 pN for an acoustic intensity of 10 W cm^{-2}, an acoustic frequency of 5 MHz and a particle diameter of 5 μm.

In Fig. 3, the potential function U is plotted as a function of z (the axial coordinate) and r (the lateral coordinate), for different materials, assuming a Gaussian intensity distribution of the standing wave. A Gaussian distribution can be obtained if the acoustic wave is focused (see next section for more details). In the diagrams, six different sphere materials, suspended in water, are compared; metal (a), glass (b), polystyrene (c), oil (d), polyethylene (e) and rubber (f). The positions of the potential wells and the shape of the potential around the wells depend on the signs of the factors f_1 and f_2 (*cf.* eqn (3)). From a material's point of view, the signs of f_1 and f_2 are determined by the density and the compressibility of the sphere and medium. As a rule of thumb, a sphere with higher density than the medium is trapped in the pressure nodes (*cf.* Fig. 3a–c) and a sphere with lower density than the medium is trapped in the pressure antinodes (*cf.* Fig. 3d). However, some materials have a more complicated potential function. In Fig. 3e, polyethylene, which has lower density and higher sound velocity than water, does not have any stable potential wells. Here, the lateral force component is directed away from the z axis for all z. Thus, stable trapping of such a material is impossible. More favorable is a potential like rubber's (*cf.* Fig. 3f), where the lateral component is attractive towards the z-axis independently of z. Most rubber materials have higher density than water, but lower sound velocity. A

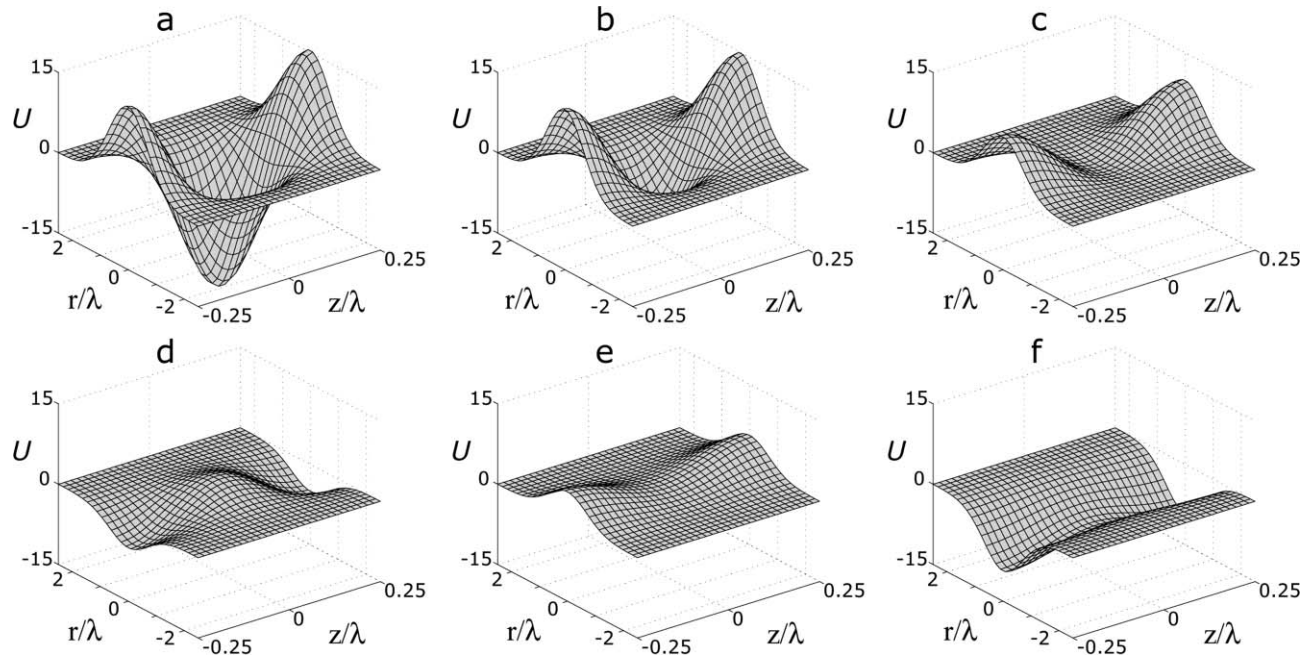

Fig. 3 The force potential U (in arbitrary units) on a spherical object, for a standing wave with a Gaussian profile propagating along the z-axis. The potential is calculated for six different sphere materials; an ideal rigid material, *e.g.*, metal (a), glass (b), polystyrene (c), oil (d), polyethylene (e) and rubber (f). A pressure node is located at position $z/\lambda = 0$, and two velocity nodes are found at positions $z/\lambda = -0.25$ and 0.25. The potential is repeated in half-wavelength intervals (*i.e.*, $z/\lambda = z/\lambda - 0.5$). The variance of the Gaussian distribution is arbitrarily chosen, and the diagrams should only be used for qualitative comparison of the shape of U between different materials.

nice application of USW manipulation based on the different force fields obtained from objects with different acoustic properties is separation of erythrocytes from lipids in whole blood.[27] In a microfluidic system, the erythrocytes are driven to the pressure node (*cf.* Fig. 3c), while lipid embolies are driven to the pressure antinodes (*cf.* Fig. 3d).

Most bead-based assays employ polystyrene spheres (latex spheres), mainly due to their availability and biocompatibility. As shown in Fig. 3c, the lateral force component in the pressure nodes for polystyrene is very weak in comparison to the axial component, even if the sound field is highly focused. Another problem is that the lateral force in between the pressure nodes is much steeper than in the pressure nodes, and also directed away from the z axis. Therefore, a sphere initially located in the pressure antinode may first move away from the z axis, simultaneous with the axial movement. When the sphere enters the pressure nodal plane, there is a risk that it is too far away from the z axis for the weak lateral force to drag it back to the potential well. A more rigid sphere, *e.g.*, a glass sphere or a metal sphere (*cf.* Fig. 3a–b), has stronger attractive lateral forces in the pressure nodes, making them more suitable for three-dimensional trapping and manipulation. However, even if the lateral shape of the potential function is not optimal for latex, it is often advantageous to employ latex in bead-based assays due to the relatively slow gravitational settlement, which keeps them in homogenous suspended phase during the assay incubation time.

In the theoretical treatment given above, the origin of the radiation force is due to the interaction between the scattered field from a single sphere and the incident (primary) acoustic field. However, when two or more spheres are present in the acoustic field, the total incident field on one of the spheres includes both the primary field and the scattered field from the other spheres. The contribution to the acoustic radiation force due to the scattered field from a nearby sphere is called the acoustic interaction force, $F_i(z)$, and is given by[34]

$$F_i(z) = 4\pi a^6 \left[\frac{(\rho-\rho_0)^2(3\cos^2\theta-1)}{6\rho_0 d^4} v^2(z) - \frac{\omega^2\rho_0(\beta-\beta_0)^2}{9d^2} p^2(z) \right], \quad (7)$$

where a is the radius of the two spheres, d is the center-to-center distance between the spheres, θ is the angle between the centerline of the spheres and the propagation direction of the incident acoustic wave, β and β_0 are the compressibilities of the sphere and the host medium, respectively, ω is the angular frequency of the acoustic wave, $v(z)$ is the particle velocity amplitude and $p(z)$ is the acoustic pressure amplitude. The sign convention defines a positive force to be repulsive, while a negative force is attractive.

An interesting phenomenon in many standing-wave traps is the formation of compact, two-dimensional and single-layer particle aggregates.[17,35,36] This can be explained by the two well-compatible force fields, the primary force, $\boldsymbol{F}$ (eqn (5)), and the secondary force, F_i (eqn (7)). In a typical application, suspended particles move initially in the direction of maximum gradient of the potential function U, (*i.e.*, parallel to the z axis). The result is a quick redistribution of all particles into the pressure nodal planes. Once inside these planes, the particles move slower in the lateral direction (towards a minimum of U) due to the weaker lateral gradient (*cf.* Fig. 3). Simultaneously, interaction forces, F_i, become significant when the particle spacing is of the order of the particle size. Interestingly, the second term in eqn (7) vanishes in the pressure nodes, and the remaining first term has a magnitude and direction dependent on the orientation of the particles (the angle θ). In or near the pressure nodes, this term is repulsive when the spheres are lined up in the direction of the acoustic wave ($\theta = 0^\circ$), and attractive when the spheres are perpendicular to the acoustic wave ($\theta = 90^\circ$). Thus, the interaction force strongly contributes to the formation of stable single-layer aggregates perpendicular to the propagation direction of the acoustic wave.

Instrumentation and resonator design

The fundamental tools needed to produce a resonant ultrasonic standing wave are a sound source and a cavity of proper dimension. The sound source is typically an ultrasonic transducer based on *e.g.*, lead zirconate titanate (PZT) piezoceramics.[37] In the simplest case, the cavity should consist of two plane and parallel surfaces that have high acoustic reflectivity and that are separated by a multiple of half the acoustic wavelength. Such a plane-parallel resonator design (*cf.* Fig. 4a) is the most widely used in USW applications.[38] The frequency of USW manipulation in liquid suspensions typically falls in the range 1–10 MHz. For a one-node trap, the width of such a half-wave resonator is 75–750 μm (assuming a sound velocity in water of $\sim$1500 m s^{-1}). This is one of the reasons for the high compatibility of USW technology in microfluidic devices, since any microfluidic channel with a well-defined rectangular cross section, hard material (*e.g.*, silicon) and width in the range >75 μm, can be used as a USW resonator. It is also possible to superpose standing-wave fields in several directions.[14,31,39] For frequencies higher than 10 MHz, absorption that causes acoustic streaming[40] is the limiting factor for high sound intensities, and for frequencies lower than 1 MHz, high pressure amplitudes may cause cavitation.[41] Thus, there is a suitable frequency window between 1–10 MHz, where relatively high acoustic intensities can be employed with low streaming and without occurrence of cavitation. In this frequency range, particles with sizes in the range 10^{-7}–10^{-4} m can be manipulated. In addition, several ways exist to minimize the streaming problem, *e.g.*, by

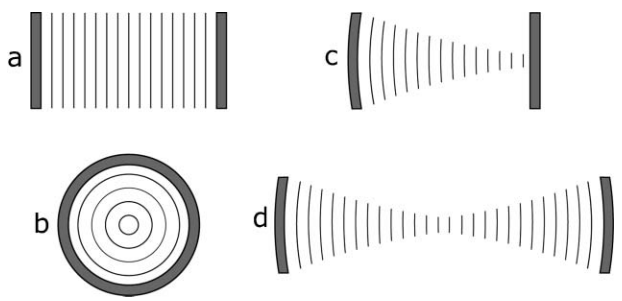

Fig. 4 (a) The plane-parallel resonator. (b) The cylindrical resonator. (c) The hemispherical resonator. (d) The confocal resonator.

shielding the streaming by the use of microchannels with smaller size than the acoustic wavelength.[16]

As discussed in the theory section, the lateral acoustic radiation force is often low in comparison to the axial force, at least two orders of magnitude lower for the plane parallel resonator. Higher lateral forces and higher stability of the trap can be obtained if focusing resonators are employed. Typically, the lateral force is one order of magnitude weaker than the axial component of the radiation force in a focusing resonator arrangement.[21] The different designs of focusing resonators are illustrated in Fig. 4b–d. The cylindrical geometry[42] is the most simple, but limits the visual access to the reaction chamber. In comparison to the confocal arrangement,[21] the hemispherical resonator is easy to align and may be operated in either a focusing mode,[16] or in a near-plane-parallel mode but with higher lateral stability.[17] The reflecting boundaries of a resonator are typically quarter-wavelength thick layers of glass or metal.[38] Such hard materials with high acoustic impedance and low acoustic absorbance are preferable to use as acoustic reflectors. However, if the thickness of the reflector is thin, carefully matched with the wavelength and backed with air, almost any material can be used, *e.g.*, plastics.[17] Most often, one of the reflectors also serves as the ultrasound source (*e.g.*, a transducer combined with a coupling layer),[38] but in some cases the transducer is not part of the resonator.[25] The resonances are found either by tuning the frequency of the transducer[22] or by tuning the resonator length in modular designs.[17] Accurate modeling of multilayer resonators can be used for optimization of the resonator design, *e.g.*, for optimization of the energy deposition in the fluid layer and for prediction of the node positions and the resonance frequencies.[43,44] For example, even if the distance between the nodes in a multilayer resonator is always half the acoustic wavelength, there is a possibility of placing the nodes at arbitrary positions relative to the boundaries of the fluid layer by matching the layer thicknesses.[45]

USW manipulation in bead-based assays

One of the first biological applications of USW manipulation was introduced in the late 1960s by Nyborg, who studied the interaction between a cell membrane and steady-state non-linear acoustic fields.[46] However, it was not until the 1980s when USW applications became widespread, first with air-borne acoustic levitation,[47] and later with separation of particles in suspensions.[48] For the purposes of this paper, however, we will concentrate on applications of USW manipulation in bead-based assays and discuss the possibility of miniaturization. A more general review of USW applications is found in, *e.g.*, ref. 14.

Today, bead-based assays are often divided into *homogeneous* and *heterogeneous* assays. One of the most widely spread heterogeneous assays is the ELISA assay (Enzyme-Linked Immunosorbent Assay). Significant for an ELISA assay is the need for separation of the solid phase (*e.g.*, antibody-coated beads) from both unbound analyte and unbound label. This requires at least two washing steps, which makes the assay complex and labor-intensive. In general, the sensitivity of ELISA tests is in the pM-range.[49] A bead-based homogeneous assay is an assay where the binding reactants (*i.e.*, the receptor-coated beads) and the analyte-containing sample is mixed, incubated and detected in bulk solution without the need for any separation steps. Such single-step, separation-free assays have the advantage of being more simple and straightforward, which results in low costs, fast solution-phase kinetics and reduced test time. In addition, homogeneous assays are more suitable for miniaturization due to low sample volume and low waste associated with the separation-free format. Here, we will focus on assay formats that have been enhanced by ultrasound, namely, agglutination-based assays (the agglutination assay and the doublet assay) and assays performed on single beads (the singlet assay).

I. Bead-based agglutination assays

The first bead-based homogeneous assay was proposed already in the 1950s, with the invention of the latex agglutination test (LAT) by Singer and Plotz.[50] The idea was to transfer the natural biological process of cell coagulation to synthetic latex beads. By coating the beads with antibodies, coagulation, or agglutination, occurred in the presence of an antigen, resulting in a turbid precipitation of aggregated beads (*cf.* Fig. 1a). LAT has long been popular in point-of-care tests for diagnostic purposes due to its simplicity, low cost and speed. During the last decade there has been over 400 publications in medicine and veterinary journals where LAT was employed, and more than 300 different biomolecules can now be detected by LAT.[51] In its simplest format, the sample is placed on a test slide and the agglutination is observed visually as a qualitative ''yes/no'' indication. Such a simple test that is familiar to most people is a standard pregnancy test, where beads coated with human chorionic gonadotropin (HCG) is mixed with a drop of urine. An extension of the LAT slides is agglutination assays based on the measurement of scattered or absorbed light. These methods allow for quantitative monitoring of the analyte concentration by measuring forward scattered (turbidimetry)[52] or side scattered (nephelometry)[53] light through the test tube. Typically, small beads in the size range 0.01–0.8 μm are used. Another quantitative approach is to use larger beads ($\sim$1 μm) and particle counting detectors based on light scattering measurements combined with flow cells.[54] These systems monitor the reduction in counting rate in a flow cell when the particles are agglutinated, or the number of unagglutinated particles by light-scattering-based discrimination. Other light scattering instruments based on low-angle light scattering have been used for investigation of particle aggregation.[55] Here, the number of particles per cluster has been determined for particles with size smaller than the wavelength. More recently, flow cytometry has been used for latex agglutination detection, where the combination of scattered light and fluorescence also allows for multiplexing.[56] This method has also been introduced in a microfluidic device.[57] However, most agglutination tests suffer from low sensitivity with detection limits in the nM-range.[49] The limiting factors are mainly the relatively high bead concentrations needed for sufficiently high particle collision rates, and non-specific agglutination (NSA) of beads. These factors will be described in more detail below.

II. USW enhancement of bead-based agglutination assays

Ultrasound has long been used for enhancement of agglutination assays.[15] The basic idea is to increase the probability of bead collisions by the use of ultrasonic forces, instead of relying on Brownian motion, gravity or microvortices produced by agitation of the sample. Initially the method was applied to enhancement of a haemagglutination assay for the detection of Hepatitis B virus.[58] In this device, erythrocytes were agglutinated in a glass capillary by a 1 MHz plane-parallel USW resonator, and the results were compared with a conventional microwell plate assay. The same device, but operating at 3 MHz, was also employed for improved detection of *Legionella pneumophilia* by agglutination in a bacterial cell suspension.[59] In both investigations, the standing-wave field was formed by reflection in the upper interface between the liquid sample and air. Later, several commercially available test kits based on cell, bacteria or latex agglutination were investigated by USW enhancement in a multiplexed format.[60] The slightly modified device used here is depicted in Fig. 5. A cylindrical 2 MHz USW resonator creates forces in the center of the cavity with magnitude $\sim$100 times higher than off-axis forces. In the center of the cavity, a 2 mm inner-diameter glass capillary is placed that contains multiple sample plugs separated by air spaces. The $\sim$50 μl volume sample plugs are placed one-by-one in the middle of the reaction chamber and sonicated, resulting in concentration of particles into the cylindrically shaped pressure nodes followed by sedimentation of agglutinated particles to the bottom of the meniscus (the interface between the sample plug and the air space). The LAT kits tested with USW enhancement showed firstly improvement in speed (between one and two orders of magnitude).[60] However, by diluting the reactants (*i.e.*, the bead concentration), an increase in sensitivity (between one and three orders of magnitude) was also observed.[61] The USW device shown in Fig. 5 has been used to demonstrate improvement in speed and sensitivity for a variety of different analytes of diagnostic interest,[62–72] and compared with alternative methods such as PCR[67] and immuno-gold lateral flow test.[70] The same technique has also been used for quantification of analyte concentration, either by measuring the aggregate size with microscopy-based image analysis,[73] or by turbidimetry.[68] A simplified instrument, based on a free sample droplet placed on a piezo-ceramic wafer, has demonstrated USW-enhancement in a LAT for diagnosis of tuberculosis.[74] A summary of different USW enhanced LATs, including the analytes, reagents and detection methods used and their sensitivity, is given in ref. 15. In the clinical context, USW enhancement in LAT detection of meningococcal antigen has received the most attention because of the urgent need for rapid diagnosis of aggressive bacterial meningitis.[75] This clinical application has resulted in a commercial instrument, Immunosonic (Electro-Medical Supplies, Wantage, UK).

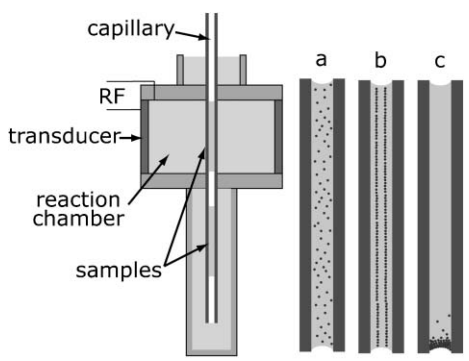

Fig. 5 The device for USW enhancement of bead-based agglutination assays. The sample of analyte and beads is placed in a capillary tube, and the capillary is placed along the axis of a cylindrical USW resonator. The sample volume in the reactor (a) is sonicated, resulting in concentration of beads into the pressure nodes (b), followed by sedimentation of aggregated beads onto the bottom meniscus (c). Figure adapted from ref. 60.

Effort has been made to investigate the lowest limit of detection that can be obtained by USW enhancement in agglutination assays. Several parameters are important for optimizing the sensitivity, *e.g.*, bead size, bead concentration, bead material, bead capacity (receptor density) and buffer composition.[51] Without USW enhancement, smaller bead size would lead to higher bead collision rate, but smaller beads also results in smaller aggregates that are more difficult to detect. Therefore, the bead size must be optimized for each agglutination assay and detection method. In USW-enhanced LATs, a decrease in detection limit with increased bead size has been reported.[76] The bead concentration (proportional to the receptor concentration) is the parameter of greatest importance for the sensitivity. Lower bead concentration directly leads to higher sensitivity since the ratio of occupied to free receptors on each bead increases (and thus, the probability of specific crosslinking of beads at collisions). However, lower bead concentration also results in slower speed of the assay. Under such conditions, USW will lead to enhancement in both speed and sensitivity, due to an increased probability of bead collisions per time unit, as well as an increased probability of specific cross-linking of beads at each collision. However, a general problem that is present in any agglutination assay is non-specific agglutination (NSA).[77] The mechanism of NSA is complex, where unspecific colloidal forces such as van der Waals, hydrophobic and electrostatic forces compete with the specific antibody–antigen interaction force (where the specific forces often have the same physical origin as the unspecific forces). In USW enhanced LATs, NSA has been suppressed by the use of silica beads instead of latex.[76] Silica has generally higher colloidal stability in water due to the more hydrophilic nature of silica compared to latex. In addition, silica is also much more suitable for USW manipulation than latex due to higher density and compressibility (*cf.* Fig. 3b–c). Detailed calculation and experimental verification have shown that silica beads, compared to latex, (i) experience higher primary acoustic forces (eqn (5)–(6)),[76] (ii) are pushed closer together in the pressure nodes by higher attractive van der Waal's forces and higher ultrasonic interaction forces (eqn (7))[76] and, (iii) can be retained in the pressure nodes even if acoustic streaming occurs.[78] Interestingly, acoustic streaming is also more suppressed if a square-shaped microchannel is employed instead of a cylindrical microchannel.[78] This observation is of importance for all USW applications in the lab-on-chip format.

The major drawbacks with a bead-based agglutination assay are the poor sensitivity and the qualitative nature of the assay.[79] Even if USW enhancement can increase the sensitivity of LATs by several orders of magnitude, the lowest reported detection limit is in the range of 10^{-11} M (for a model system with streptavidin-coated silica beads and biotinylated bovine serum albumin as the analyte).[76] The reason for the difficulties of using LATs for quantitative measurements lies in the principle of agglutination. A specific crosslinking of two beads requires that an analyte–receptor complex on one bead is bound to a free receptor on the other bead. Thus, the probability for crosslinking will increase with the analyte concentration up to a level where half of the receptors on the beads are occupied. At even higher analyte concentrations, the probability will instead decrease, resulting in inhibition of the agglutination. For example, a low analyte concentration that causes 5% receptor occupancy and a high analyte concentration that causes 95% receptor occupancy will result in exactly the same amount of agglutination. This effect, the hook-effect or the prozone phenomenon,[80] can be suppressed to some extent with USW enhancement, but not eliminated.[66] However, USW-enhanced LATs offer a simple, cheap, fast and reliable alternative to more advanced methods for a lot of diagnostic purposes. Furthermore, the method is suitable to implement in the lab-on-chip format, something that still remains to be demonstrated.

III. Bead-based doublet assays

Another approach is to measure the very initial stage of agglutination where two single beads (singlets) form a bead pair (doublet), see Fig. 1b. This technique shows promise for improved sensitivity compared to traditional agglutination assays that require the formation of larger complexes. Besides, the kinetics of initial agglutination is well understood. For example, theoretical modeling can be used to optimize a doublet assay in terms of sensitivity and dynamic range as well as to estimate the affinity, receptor surface density, sizes of the molecules and their binding sites in the immunoassay and the level of non-specific binding that is present in the assay.[56] The doublet assay has been employed in flow-through systems, *e.g.*, in capillary electrophoresis (CE)[81,82] and scanning flow cytometry (SFC).[83] The latter method is powerful for resolving the number of beads in small agglomerates, and is an extension of low-angle light scattering detection.[55] However, both CE and SFC have limited reported sensitivity ($\sim 10^{-10}$ M detection limit at best).[81] An alternative to the flow-through methods are detection methods in bulk samples. An elegant and sensitive doublet assay in bulk samples is the luminescent oxygen channeling immunoassay (LOCI).[84] The LOCI method uses two different 175 nm beads, a donor bead and a receptor bead, and monitors doublet formation by chemiluminescence. By laser-exciting the donor bead at 680 nm, ejection of single-state oxygen radicals, $^1\Delta_g O_2$, converts the laser light to emission light from the acceptor bead at 520–620 nm by a chemiluminescence reaction. Since the oxygen radical has a short diffusion range ($\sim$250 nm), emission light is only detected if the donor and acceptor have combined to a doublet during the 0.3 s reaction lifetime. The time-resolved LOCI-detection of doublets has significant potential for high sensitivity and may also monitor the reaction in real time. The reported detection limit is of the order of 10^{-13} M.[84] Finally, a simplified bead-based doublet assay has recently been reported based on counting of singlets and doublets by image analysis in fluorescence microscopy.[56] Here, pattern recognition algorithms allow for classification of singlets and doublets with high reliability even with limited image quality. The method is simple and straightforward, and has significant potential for implementation to the lab-on-chip format. High sensitivity would be possible if the method was combined with USW enhancement prior to detection.[14]

IV. USW enhancement of bead-based doublet assays

Ultrasound has been suggested for size-selective separation of doublets from single beads.[16,85] Very high size selectivity can be obtained by combining the USW technique and an electro-osmotic flow.[85] This device, illustrated in Fig. 6, is built around a capillary electrophoresis system, and the separation method also includes sample enrichment. In a well-defined segment of the capillary, starting from the acoustic reflector, doublets may be retained in the pressure nodes of the standing wave while single beads elude the trap. The separation mechanism is based on competition between the acoustic force and the viscous fluid drag from the electro-osmotic flow. The system works as a high-precision filter where the ''pore size'' is carefully controlled by the acoustic intensity. However, even if the size selection and sample enrichment is very efficient, the method does not enhance the agglutination mechanism. Therefore, the sensitivity is not better than $\sim$nM.[14] On the other hand, the method has high potential for miniaturization, since only the ultrasound source is macro-scaled. In addition, higher sensitivity could be obtained if ultrasound is used in two steps, first to enhance the doublet formation (as described in Section II) and then to enrich and detect doublets (as described here). Finally, it should be mentioned that a similar method for size-selection and USW trapping inside a capillary has been proposed, based on transverse acoustic waves or a

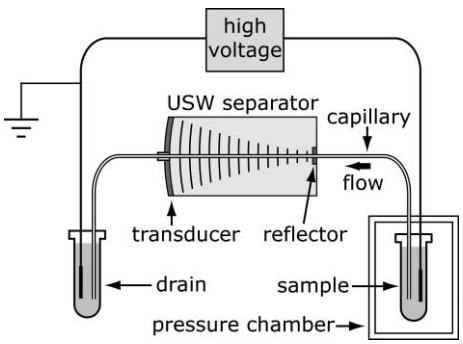

Fig. 6 The device for USW doublet detection in a microfluidic capillary. The sample is injected in the USW trap by an electro-osmotic flow, generated by a capillary electrophoresis system. Inside the capillary USW trap, doublets may be trapped, retained, enriched and separated from single beads by the competition between acoustic forces and viscous forces from the fluid drag. The standing wave is longitudinally coupled into the capillary by a hemispherical resonator aligned parallel to the capillary. Figure adapted from ref. 85.

combination of bulk and flexural acoustic modes.[86,87] The latter method is called "ultrasonic chromatography", with reference to a similar method ("optical chromatography") based on optical forces.[88]

V. Bead-based singlet assays

The singlet assay, shown in Fig. 1c, differs from the agglutination assay and the doublet assay since it is performed on individually antibody-coated beads in combination with a labeled second antibody. The label, or tag, could be an enzyme or a fluorescent, a radioactive or a chemiluminescent molecule. In principle, the assay can be performed on a single bead, even if many beads usually are measured to obtain a statistically significant result. When the beads are mixed with the sample and the label, the analyte is sandwiched between bead-immobilized capture antibodies and the labeled molecule. The amount of label on each bead could then be used as a measure of the analyte concentration in the sample. The singlet assay is particularly suitable for miniaturization, since very low sample volumes ($\sim$µl or sub-µl) can be used. However, the main problem in singlet assays is the handling of individual beads. Therefore, the singlet assay can be efficiently improved by the combination with USW manipulation. This is a novel approach in bead-based assays that has potential for ultrahigh sensitivity.

The singlet assay has long been employed in methods based on flow cytometry.[89] Here, scattered light and fluorescence are used to discriminate beads on the basis of both the size and the color of the bead. Beads encoded with various amounts of several fluorophores has resulted in a novel technological concept, suspension array technology (SAT),[6] and this method has also been commercialized (*e.g.*, Luminex Corporation, Austin, TX, USA). Characteristics for flow cytometric methods are very high throughput but limited sensitivity. Another approach is to scan a laser focus in a bulk solution instead of using a flow-through system. This is performed in two-photon excitation (TPX) technology.[90] Here, the fluorescence of two-photon excitation in bulk solution is measured in a small confocal volume element, by employing the singlet assay. Since two-photon excitation is a quadratic process with respect to the illumination intensity, only fluorophores in the clearly restricted vicinity of the laser focus are excited. This results in efficient suppression of the background noise. In a TPX singlet assay, the laser focus is scanned in the bulk sample, searching for beads. When a bead appears in the focus, the scanner is stopped and the TPX fluorescence is measured. An advantage using this method is the possibility of monitoring the reaction kinetics, since the measurement can be performed simultaneously with the incubation. Typically, the detection limit is in the pM range. The TPX concept has been commercialized by Arctic Diagnostics (ArcDia TPX, Arctic Diagnostics Oy, Turku, Finland). A similar approach to TPX technology is confocal microscopy-based techniques. In "macro-confocal" laser-scanning fluorescence detection, a 100 µm axially elongated laser beam is automatically focused and laterally scanned on the bottom of a microplate well.[91] The fluorescence is measured on beads on the bottom of the well, and the "macro-confocal" concept also allows for suppression of the background noise from unbound tracer antibodies. The reported sensitivity of this method is similar to the sensitivity of TPX technology ($\sim$pM). Both TPX and confocal detection techniques employ a single-step assay, where the detection is made directly without the need for washing away unbound tracer reactants.

Several non-fluorescent and sensitive singlet assays also exist, *e.g.*, scintillation proximity assay (SPA)[92] and electrochemiluminescence (ECL).[93] ECL especially is considered as an ultrasensitive assay with sub-pM detection limits. The ECL assay employs magnetic beads and has been commercialized by *e.g.*, Igen Inc. (Origen™, Igen Inc., Gaithersburg, MD, USA) and Roche Diagnostics GmbH (Elecsys™, Roche Diagnostics GmbH, Mannheim, Germany).

One of the most important factors for the sensitivity of a singlet assay is the concentration of beads in the sample. This is a consequence of the concentration of bead-immobilized capture antibodies in relation to the analyte concentration. In 1989, Ekins proposed the concept of the ambient analyte immunoassay, where much higher sensitivity can be obtained if the concentration of capture antibody is very low ($<0.01/K$, where K is the affinity constant of the binding reaction).[94] In ambient analyte conditions, the analyte and tracer concentrations are much higher than the capture antibody concentration, which results in a fractional occupancy of the capture antibody binding sites that is dependent on the concentration of analyte only. For the bead-based singlet assay, ambient analyte theory proposes that if the concentration of beads is decreased, the amount of analyte and tracer on each bead increases, resulting in a lower detection limit. Ekins used this concept in microspot array technology,[95] where a minute amount of capture antibodies in small spots on a solid surface allows for ultrahigh sensitivity in combination with confocal fluorescence detection. Ekins' theory is one of the best examples of the power of miniaturization.

VI. USW enhancement of bead-based singlet assays

USW manipulation has been used with a single-step, homogeneous singlet assay combined with confocal laser-scanning fluorometry.[17] This technique shows promise for ultrahigh sensitivity; preliminary results indicate a possible detection limit of the order of fM for a human thyroid stimulating hormone (hTSH) singlet assay.[17] The system, depicted in Fig. 7, consists of three parts: an inverted confocal microscope, a 96-well microtiter plate and a miniature focused transducer assembly (FTA). The FTA and the optically transparent bottom of the microplate form a USW resonator in a hemispherical arrangement (*cf.* Fig. 4c), where the resonator length can be carefully tuned into resonance by axial positioning of the FTA. First, the sample is placed in one of the wells in the microplate and incubated with the beads and label. Then, the FTA is placed in the well and aligned into resonance. At resonance, the beads in the sample are driven into the pressure nodes of the standing wave. Eventually, the beads are arranged in compact, hexagonal and two-dimensional aggregates in several horizontal planes, each separated vertically by a distance corresponding to half the acoustic

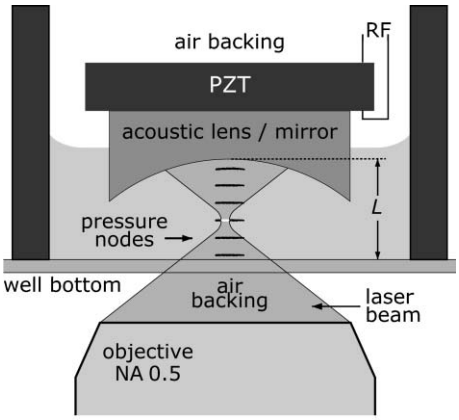

Fig. 7 The device for USW enhancement of bead-based singlet assays. A miniature 4 MHz focused transducer assembly (FTA) is submerged into one of the microplate wells containing the sample. The USW resonator is formed by the FTA and the bottom of the microplate well. The USW resonator length, L, is tuned into resonance, and the beads are trapped and enriched in compact two-dimensional aggregates in the pressure nodes. Finally, the confocal laser-scanning fluorescence system scans horizontally each aggregate one-by-one. Figure adapted from ref. 17.

wavelength. The mechanism of the formation of such two-dimensional aggregates is described in the theory section. The fluorescence from the planar aggregates is detected by the confocal laser-scanning system. The geometry of the USW-trapped aggregates is perfectly matched to the scanning area of the confocal microscope. The vertical and lateral positions of the centerpoints of the pressure nodes are predefined and in principle, the scanning unit of the microscope can be pre-programmed to scan each aggregate one-by-one.

The idea of using USW manipulation in a singlet assay is to improve the sensitivity according to Ekins' theory of ambient analyte conditions. By reducing the concentration of beads in the microplate well, a higher fluorescence signal can be measured from each bead. However, when the bead concentration is reduced, the probability per time unit of finding a bead when scanning the laser focus in the sample is significantly reduced. The USW method is used here for bead enrichment into the scanning area of the confocal detection system. The system shows a remarkable high enrichment factor. Typically, the beads in a 100 μl sample containing $\sim$2500 beads (corresponding to a volume fraction of $\sim 10^{-7}$), are rearranged into 6 aggregates each containing $\sim$50 beads (*cf*. Fig. 8).[17] The volume of each aggregate is $\sim$150 fl, and since $\sim$10% of the beads are trapped the enrichment factor is between 10^6 and 10^7. This can be compared with sedimentation or centrifugation, which has an enrichment factor of maximum 10^3 for a similar sample. However, at very low bead concentrations, the affinity of the assay is the limiting factor. This is illustrated in Fig. 9, where the amount of analyte on each bead is calculated as a function of the bead concentration for the hTSH assay. The calculation is based on the theory presented in ref. 56. Without USW enhancement, the confocal detection system can handle samples with bead concentrations $>10^6$ ml^{-1}. When the bead concentration is decreased, the gain in signal from each bead is increased up to a level where an

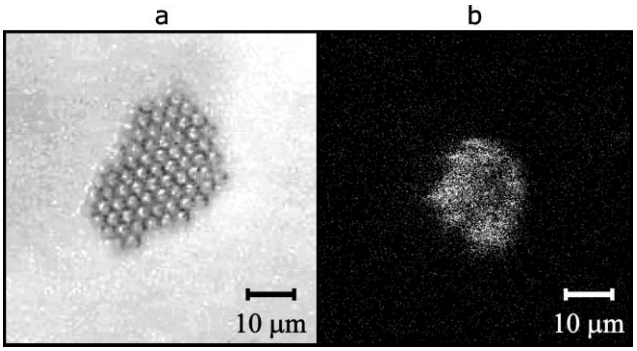

Fig. 8 (a): Reflected light from 65 beads trapped in the middle of the $\sim$40 μL active sample volume. This pressure node is the 4th from the transducer, corresponding to a distance of $\sim$0.6 mm from the transducer, and approximately the same distance from the bottom of the microplate. (b): Fluorescence light from a 10 s long confocal scan of approximately 20 trapped beads. The image is taken from a human thyroid stimulating hormone (hTSH) assay experiment with an analyte concentration of 70 pM. Images adapted from ref. 17.

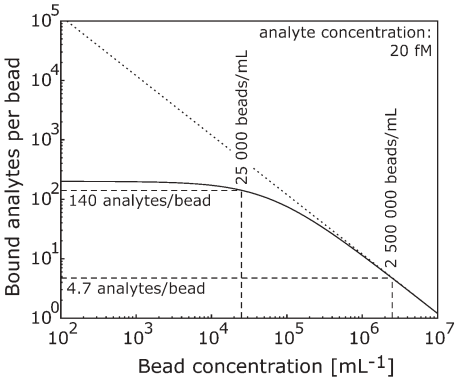

Fig. 9 Calculation of the average amount of analyte bound to each bead at equilibrium as a function of the bead concentration for the human thyroid stimulation hormone (hTSH) assay. In the calculation, a constant analyte concentration of 20 fM (the experimental detection limit) is used to illustrate the dependence of signal-to-background of the detection system to the concentration of bead-immobilized receptors. The two bead concentrations that can be handled by the system with (2.5×10^4 ml^{-1}) and without (2.5×10^6 ml^{-1}) USW enrichment are marked in the diagram. Typically, $\sim$100 analyte molecules can be discriminated from the background if the amount of analyte and label (tracer antibodies) bound to each bead is assumed to be equal.

affinity-related saturation effect occurs. Besides, dilution of the beads also results in a slower assay. However, bead samples diluted 2 or 3 orders of magnitude still results in amplified signal and reasonable incubation times. This indicates that the theoretical detection limit for the hTSH assay is at the low fM-level, corresponding to the detection of 10–100 tracer fluorophores per bead.

Another approach for USW enhancement of a singlet assay in a microfluidic chip has been demonstrated by Lilliehorn and coworkers.[18] They use a microfabricated flow-through system with parallel microchannels and microtransducers integrated in the chip, see Fig. 10. In principle, this system could be used as a flexible bead-based microarray chip, where small

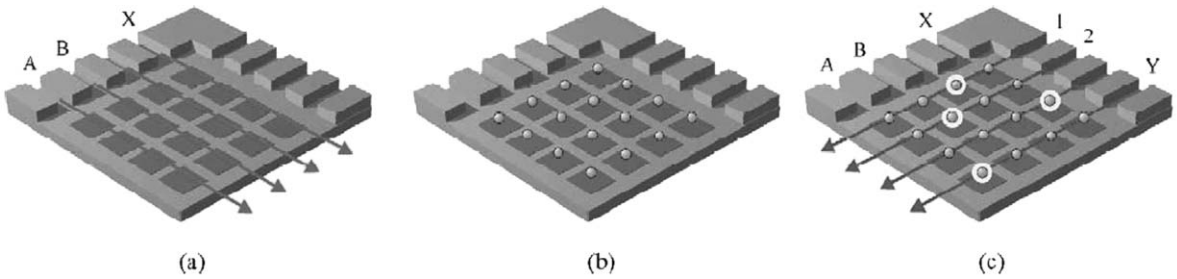

Fig. 10 Illustrations of the concept of dynamic arraying showing insertion of the solid phase of different specificity (a) through inlets (A, B, …, X), trapping of antigen specific bead clusters using the ultrasonic transducer array (b) and perfusion/incubation of sample (c) through inlets (1, 2, …, Y) followed by fluorescence read-out. Figure reprinted from ref. 18 with permission from Elsevier.

agglomerates of beads can be trapped above each transducer element before the sample is flushed through the chip. This concept of dynamic arraying of beads is very interesting for multiplexing by USW manipulation, and is also fully integrated in a lab-on-chip system that employs μl sample volumes. However, in comparison to USW enrichment in microtiter plates, this method is more complex and more difficult to make ultrasensitive since the system is not designed for handling of samples with very low bead concentrations. Finally, it should also be mentioned that USW enhancement has been reported in a fiber-optic biosensor for the detection of *Salmonella* cells.[96] Here, latex beads are used to improve the enrichment of the cells into the pressure nodes, by the formation of cell-bead aggregates prior USW operation. Similar approaches have also been reported for improved detection of bacterial spores or cells, where USW manipulation is used for particle deposition to an immunosensor surface.[28,97,98]

VII. Other field-assisted manipulation methods in bead-based assays

Other reported methods for field-assisted enhancement of bead-based assays exist, based on other techniques than ultrasound. For example, LATs have been employed with magnetic beads in a microfluidic format.[11] In the presence of a magnetic field, superparamagnetic beads form linear aggregates, and the length and number of aggregates can be used as a measure of analyte concentration. The authors claim a detection limit of 10 fM for a biotin–streptavidin-based assay. However, this very high sensitivity needs to be verified by more experiments. Other field-assisted methods include electric field-enhanced LATs,[99] dielectrophoresis-controlled adhesion of beads to electrode microarrays for affinity assays[100] and doublet detection by optical chromatography.[88]

Conclusion and summary

The performance and characteristics of the different USW techniques for enhancement in bead-based assays is compared in Table 1. The most established method is USW enhancement in latex agglutination tests (LATs), which has resulted in thorough investigations, clinical evaluations and a commercial device. The strength with this technique is that it employs an inexpensive, simple and accessible assay, where USW enhancement makes a significant difference in both speed and sensitivity. However, the drawback is that more advanced alternative methods, *e.g.*, PCR, are often superior even if LATs are faster. On the other hand, USW enhancement in LATs still has potential for improvements, *e.g.*, miniaturization that can increase the level of automation and detection of doublets instead of large aggregates. Detection especially is problematic in qualitative LATs, since the interpretation of agglutination is often considered to have an element of subjectivity.[79] The second proposed method, USW-based separation and enrichment of doublets in capillaries, has high potential in applications where sensitive size-selection is needed, but the technique is hardly of benefit to the bead-based doublet assay. The reason is that ultrasound is only used to detect and enrich doublets that are already cross-linked, and not to enhance the agglutination mechanism. The last proposed method, USW enrichment in the singlet assay, has the highest potential for ultrahigh sensitivity. For the TSH assay, preliminary results indicate a detection limit at the low fM level. This is about 1–2 orders of magnitude lower than the

Method	USW agglutination enhancement	USW doublet detection	USW bead enrichment
Assay format	Agglutination of beads	Agglutination of beads, initial stage (doublet)	Individual beads and label (singlet)
Sensitivity	10^{-11}–10^{-9} M	$\sim 10^{-10}$ M	$\sim 10^{-14}$ M
USW frequency	2–5 MHz	8 MHz	4–10 MHz
USW resonator	Cylindrical	Hemispherical	Hemispherical and plane-parallel
Bead size	0.3–1.0 μm	1–5 μm	3–7 μm
Detection	Microscopy, image analysis, turbidimetry	Size-selective USW separation	Confocal laser-scanning fluorometry, fluorescence microscopy
Miniaturization	Possible	Yes (microfluidic capillaries)	Yes (microwell plates and microfluidic chips)
Potential improvements	Detection of the initial stage of agglutination, miniaturization	Combine with USW agglutination enhancement	Smaller beads, amplified labels, multiplexing

detection limit of standard ELISA methods[101] and equivalent to the detection limits of some of the most sensitive methods that are commercially available.[102] Furthermore, the USW method is cost-effective by the use of transducers made of ~1-Euro PZT wafers, disposable commercially available microtiter plates and confocal microscopes that are available at many laboratories and clinics. However, the reported results are still of a preliminary nature. Several improvements can be made, both instrumentation-related (optimization of the transducer–microplate system, and even further system miniaturization[103]) and assay-related (*e.g.*, optimization of the assay in terms of bead size, bead capacity, and choice of label). The dynamic arraying concept opens new possibilities for miniaturization and parallelization, and should be further investigated for higher sensitivity. Finally, when comparing the USW methods in the agglutination assay and the singlet assay, it is important to note that the hook-effect, discussed above for the former method, is present in any single-step, homogeneous assay including the singlet assay. However, the effect is of less importance for the singlet assay. The reason is the higher flexibility resulting from the different nature of the solid phase capture antibodies (*i.e.*, the beads) and the label (*i.e.*, the tracer antibodies). In the agglutination assay, the solid phase and the label are one and the same (*i.e.*, the beads). In addition, the agglutination assay has a more complicated non-specific binding, which limits the sensitivity. For the singlet assay, the level of non-specific binding is most often very low or even absent due to the low concentration of the label.[104] Furthermore, the background interference in complex biological samples, which may compromise the sensitivity, has not turned out to be a major problem.[105]

Another approach for improved sensitivity in bead-based assays, that can readily be implemented in USW-enhanced assays for even further sensitivity enhancement, is to employ different techniques for amplification of the label. Such techniques show promise for extremely high sensitivity, even at the sub-fM level.[106] In principle, the sensitivity gain due to USW enhancement and due to label amplification is not interfering and can therefore be multiplied. The amplification is often based on the use of nanobeads as carriers of the label. In such an assay, each bound analyte molecule on the solid phase capture bead is represented by a large amount of nanobead-immobilized label, where the label could be either DNA-code (oligonucleotides)[106] or fluorophores.[104,107] The fluorescence-based nanobead label is the most interesting for potential use in a single-step homogeneous USW-enhanced singlet assay, due to its simplicity.[104]

It is interesting to compare the positive attributes of suspension array technology (SAT)[6] and microspot array technology,[9] with the attributes of USW enhancement in the singlet assay.[17] SAT offers multiplexing in a single microplate well and fast solution-phase kinetics with an assay performed on suspended beads. On the other hand, microspot array technology offers ultrahigh sensitivity by the use of very small amounts of capture antibodies arranged in small spots on a planar surface, in agreement with Ekins' ambient analyte theory.[94] In this context, USW enhancement of the singlet assay can be considered as a microspot array performed in the suspension array format. With the ultrasound method, the highly diluted beads that are suspended in the sample are rearranged and enriched into microspots at well-defined positions in the pressure nodes of the standing wave. First, the incubation of the assay is made in the homogeneous format with freely suspended beads, followed by the ''USW-production'' of bead-based microspots that can be screened by the detection system. While planar microspot arrays must be prefabricated as discrete items by printing of antibodies into predefined and spatially separated microspots on the binding surface, bead-based suspension arrays have the advantage of lower production cost, higher yield and quality control since antibody-coated beads can be produced in large batches. Therefore, USW technology in bead-based assays offers a novel and versatile approach for both ultrahigh sensitivity and cost-effectiveness in the detection of different analytes of interest.

Acknowledgements

This work was supported by the Swedish Research Council for Engineering Sciences and the European Community-funded *CellPROM* project under the 6th Framework Programme, contract No. NMP4-CT-2004-500039. The authors gratefully thank Prof. Pekka Hänninen, Dr Harri Härmä, MSc. Janne Koskinen and Dr Andrei V. Chernyshev for useful discussions about reaction kinetics and detection limits in bead-based assays.

References

1 M. B. Meza, Bead-based HTS applications in drug discovery, *Drug Discovery Today*, 2000, **5**(Suppl. 1), 38–41.
2 E. Verpoorte, Beads and Chips: new recipes for analysis, *Lab Chip*, 2003, **3**, 60N–68N.
3 H. Härmä, Particle Technologies, in *Diagnostics, Technology review 126/2002*, TEKES, Helsinki, Finland, 2002.
4 P. Hänninen, A. Soini, N. Meltola, J. Soini, J. Soukka and E. Soini, A new microvolume technique for bioaffinity assays using two-photon excitation, *Nat. Biotechnol.*, 2000, **18**, 548–550.
5 H. Kawaguchi, Functional polymer microspheres, *Prog. Polym. Sci.*, 2000, **25**, 1171–1210.
6 J. P. Nolan and L. A. Sklar, Suspension array technology: evolution of the flat-array paradigm, *Trends Biotechnol.*, 2002, **20**, 9–12.
7 R. S. M. S. Karumanchi, S. N. Doddamane, C. Sampangi and P. W. Todd, Field-assisted extraction of cells, particles and macromolecules, *Trends Biotechnol.*, 2002, **20**, 72–78.
8 K. N. Baker, M. H. Rendall, A. Patel, P. Boyd, M. Hoare, R. B. Freedman and D. C. James, Rapid monitoring of recombinant protein products: a comparison of current technologies, *Trends Biotechnol.*, 2002, **20**, 149–156.
9 M. F. Templin, D. Stoll, M. Schrenk, P. C. Traub, C. F. Vöhringer and T. O. Joos, Protein microarray technology, *Trends Biotechnol.*, 2002, **20**, 160–166.
10 J. Enger, M. Goksör, K. Ramser, P. Hagberg and D. Hanstorp, Optical tweezers applied to a microfluidic system, *Lab Chip*, 2004, **4**, 196–200.
11 G. Degré, E. Brunet, A. Dodge and P. Tabeling, Improving agglutination tests by working in microfluidic channels, *Lab Chip*, 2005, **5**, 691–694.
12 T. Müller, A. Pfennig, P. Klein, G. Gradl, M. Jäger and T. Schnelle, The potential of dielectrophoresis for single-cell experiments, *IEEE Eng. Med. Biol. Mag.*, 2003, **22**, 51–61.
13 N. R. Harris, M. Hill, S. Beeby, Y. Shen, N. M. White, J. J. Hawkes and W. T. Coakley, A silicon microfluidic ultrasonic separator, *Sens. Actuators, B*, 2003, **95**, 425–434.

14 M. Wiklund, PhD Thesis, *Ultrasonic enrichment of microparticles in bioaffinity assays,* Royal Institute of Technology, Stockholm, Sweden, 2004.
15 R. W. Ellis and M. A. Sobanski, Diagnostic particle agglutination using ultrasound: a new technology to rejuvenate old microbiological methods, *J. Med. Microbiol.*, 2000, **49**, 853–859.
16 M. Wiklund, S. Nilsson and H. M. Hertz, Ultrasonic trapping in capillaries for trace-amount biomedical analysis, *J. Appl. Phys.*, 2001, **90**, 421–426.
17 M. Wiklund, M. Tirri, J. Toivonen, P. Hänninen and H. M. Hertz, Ultrasonic enrichment of microspheres for ultrasensitive biomedical analysis in confocal laser-scanning fluorescence detection, *J. Appl. Phys.*, 2004, **96**, 1242–1248.
18 T. Lilliehorn, M. Nilsson, U. Simu, S. Johansson, M. Almqvist, J. Nilsson and T. Laurell, Dynamic arraying of microbeads for bioassays in microfluidic channels, *Sens. Actuators, B*, 2005, **106**, 851–858.
19 A. Kundt and O. Lehmann, Longitudinal vibrations and acoustic figures in cylindrical columns of liquids, *Ann. Phys. Chem.*, 1874, **153**, 1.
20 E. H. Brandt, Levitation in physics, *Science*, 1989, **243**, 349–255.
21 H. M. Hertz, Standing-wave acoustic trap for nonintrusive positioning of microparticles, *J. Appl. Phys.*, 1995, **78**, 4845–4849.
22 M. Gröschl, Ultrasonic separation of suspended particles—Part I: Fundamentals, *Acustica*, 1998, **84**, 432–447.
23 E. H. Brandt, Acoustic physics—Suspended by sound, *Nature*, 2001, **413**, 474–475.
24 J. J. Hawkes and W. T. Coakley, Force field particle filter, combining ultrasound standing waves and laminar flow, *Sens. Actuators, B*, 2001, **75**, 213–222.
25 A. Nilsson, F. Petersson, H. Jönsson and T. Laurell, Acoustic control of suspended particles in micro fluidic chips, *Lab Chip*, 2004, **4**, 131–135.
26 J. J. Hawkes, R. W. Barber, D. R. Emerson and W. T. Coakley, Continuous cell washing and mixing driven by an ultrasound standing wave within a microfluidic channel, *Lab Chip*, 2004, **4**, 446–452.
27 F. Petersson, H. Nilsson, C. Holm, H. Jönsson and T. Laurell, Continuous separation of lipid particles from erythrocytes by means of laminar flow and acoustic standing wave forces, *Lab Chip*, 2005, **5**, 20–22.
28 J. J. Hawkes, M. J. Long, W. T. Coakley and M. McDonnel, Ultrasonic deposition of cells on a surface, *Biosens. Bioelectron.*, 2004, **19**, 1021–1028.
29 T. Lilliehorn, U. Simu, M. Nilsson, M. Almqvist, T. Stepinski, T. Laurell, J. Nilsson and S. Johansson, Trapping of microparticles in the near field of an ultrasonic transducer, *Ultrasonics*, 2005, **43**, 293–303.
30 F. Petersson, A. Nilsson, H. Jönsson and T. Laurell, Carrier medium exchange through ultrasonic particle switching in microfluidic channels, *Anal. Chem.*, 2005, **77**, 1216–1221.
31 A. Haake, A. Nield, G. Radziwill and J. Dual, Positioning, displacement, and localization of cells using ultrasonic forces, *Biotech. Bioeng.*, 2005, **92**, 8–14.
32 M. Wiklund, C. Günther, R. Lemor, M. Jäger, G. Fuhr and H. M. Hertz, 2005, Ultrasonic standing-wave manipulation technology integrated into dielectrophoretic chips, *Lab Chip*, 2006, **6**, submitted.
33 L. P. Gor'kov, On the forces acting on a small particle in an acoustic field in an ideal fluid, *Soc. Phys. Dokl.*, 1962, **6**, 773–775.
34 M. A. H. Weiser and R. E. Apfel, Interparticle forces on red-cells in a standing wave field, *Acustica*, 1984, **56**, 114–119.
35 J. F. Spengler and W. T. Coakley, Ultrasonic trap to monitor morphology and stability of developing microparticle aggregates, *Langmuir*, 2003, **19**, 3635–3642.
36 D. Bazou, W. T. Coakley, K. M. Meek, M. Yang and D. T. Pham, Characterisation of the morphology of 2-D particle aggregates in different electrolyte concentration in an ultrasound trap, *Colloids Surf., A.*, 2004, **243**, 97–104.
37 B. Jaffe, W. R. Cook and H. Jaffe,*Piezoelectric Ceramics*, Academic Press, London, 1971.
38 M. Gröschl, Ultrasonic separation of suspended particles—Part II: Design and operation of separation devices, *Acustica*, 1998, **84**, 632–642.
39 T. Kozuka, T. Tuziuti, H. Mitome, F. Arat and T. Fukuda, Control of position of a particle using a standing wave field generated by crossing sound beams, *Proc. IEEE Ultrasonics Symp.*, 1998, 657–660.
40 L. K. Zarembo, Acoustic Streaming, in *High-Intensity Ultrasonic Fields*, ed. L. D. Rozenberg, Plenum Press, New York, 1971, vol. 85, part 3, pp. 138–199.
41 R. K. Gould, W. T. Coakley and M. A. Grundy, Upper sound pressure limits on particle concentration in fields of ultrasonic standing-wave at megahertz frequencies, *Ultrasonics*, 1992, **30**, 239–244.
42 M. A. Grundy, W. E. Bolek, W. T. Coakley and E. Benes, Rapid agglutination testing in an ultrasonic standing wave, *J. Immunol. Methods*, 1993, **165**, 47–57.
43 H. Nowotny and E. Benes, General one-dimensional treatment of the layered piezoelectric resonator with two electrodes, *J. Acoust. Soc. Am.*, 1987, **82**, 513–521.
44 M. Hill, The selection of layer thicknesses to control acoustic radiation force profiles in layered resonators, *J. Acoust. Soc. Am.*, 2003, **114**, 2654–2661.
45 N. Harris, M. Hill, Y. Shen, R. J. Townsend, S. Beeby and N. White, A dual frequency, ultrasonic, microengineered particle manipulator, *Ultrasonics*, 2004, **42**, 139–144.
46 W. L. Nyborg, Mechanisms for nonthermal effects of sound, *J. Acoust. Soc. Am.*, 1968, **44**, 1302–1309.
47 R. R. Whymark, Acoustic field positioning for containerless processing, *Ultrasonics*, 1975, **13**, 251–261.
48 M. Gröschl, Ultrasonic separation of suspended particles—Part III: Application in biotechnology, *Acustica*, 1998, **84**, 815–822.
49 J. Baudry, E. Bertrand, C. Rouzeau, O. Greffier, A. Koenig, R. Dreyfus, L. Cohen-Tannoudji, C. Goubault, L. Bressy, L. Vincent, N. Lequeux and J. Bibette, Colloids for studying molecular recognition, *Ann. Chim.–Sci. Mat.*, 2004, **29**, 97–106.
50 J. M. Singer and C. M. Plotz, The latex fixation test. I. Applications to the serologic diagnosis of rheumatoid arthritis, *Am. J. Med.*, 1956, **21**, 888.
51 J. A. Molina-Bolívar and F. Galisteo-González, Latex immunoagglutination assays, *J. Macromol. Sci., C*, 2005, **45**, 59–98.
52 W. J. Litchfield, A. R. Craig, W. A. Frey, C. C. Leflar, C. E. Looney and M. A. Luddy, Novel shell core particles for automated turbidimetric immunoasays, *Clin. Chem.*, 1984, **30**, 1489–1493.
53 W. H. Kapmeyer, W. H. Pauly and P. Tuengler, Automated nephelometric immunoassays with novel shell core particles, *J. Clin. Lab. Anal.*, 1988, **2**, 76–83.
54 P. L. Masson, Particle Counting Immunoassay—an Overview, *J. Pharmaceut. Biomed.*, 1987, **5**, 113–117.
55 M. S. Bowen, M. L. Broide and R. J. Cohen, Determination of Cluster Size Distributions Using an Optical Pulse Particle-Size Analyzer, *J. Colloid Interface Sci.*, 1985, **105**, 605–616.
56 M. Wiklund, O. Nord, R. Gothäll, A. V. Chernyshev, P.-Å. Nygren and H. M. Hertz, Fluorescence-microscopy-based image analysis for analyte-dependent particle doublet detection in a single-step immunoagglutination assay, *Anal. Biochem.*, 2005, **338**, 90–101.
57 N. Pamme, R. Koyama and A. Manz, Counting and sizing of particles and particle agglomerates in a microfluidic device using laser light scattering: application to a particle-enhanced immunoassay, *Lab Chip*, 2003, **3**, 187–192.
58 M. A. Grundy, W. T. Coakley and D. J. Clarke, Rapid detection of Hepatitis B virus using a haemagglutination assay in an ultrasonic standing wave field, *J. Clin. Immunol.*, 1989, **30**, 93–96.
59 R. I. Jepras, D. J. Clarke and W. T. Coakley, Agglutination of Legionella pneumophilia by antiserum is accelerated in an ultrasonic standing wave, *J. Immunol. Methods*, 1989, **120**, 201–205.
60 M. A. Grundy, W. E. Bolek, W. T. Coakley and E. Benes, Rapid agglutination testing in an ultrasonic standing wave, *J. Immunol. Methods*, 1993, **165**, 47–57.
61 M. A. Grundy, K. Moore and W. T. Coakley, Increased sensitivity of diagnostic latex agglutination tests in an ultrasonic standing wave field, *J. Immunol. Methods*, 1994, **176**, 169–177.

62 M. A. Grundy, R. A. Barnes and W. T. Coakley, Highly sensitive detection of fungal antigens by ultrasound-enhanced latex agglutination, *J. Med. Vet. Mycol.*, 1995, **33**, 201–203.
63 M. P. Gualano, M. A. Grundy, W. T. Coakley, S. H. Parry and D. J. Stickler, Ultrasound-enhanced latex agglutination for the detection of bacterial antigens in urine, *Br. J. Biomed. Sci.*, 1995, **52**, 178–183.
64 P. Jenkins, R. A. Barnes and W. T. Coakley, Detection of meningitis antigens in buffer solution and body fluids by ultrasound-enhanced particle agglutination, *J. Immunol. Methods*, 1997, **205**, 191–200.
65 R. A. Barnes, P. Jenkins and W. T. Coakley, Preliminary clinical evaluation of meningococcal disease and bacterial meningitis by ultrasonic enhancement, *Arch. Dis. Child*, 1998, **78**, 58–60.
66 P. Jenkins, M. A. Sobanski, M. Gualano and W. T. Coakley, Ultrasound pre-treatment can extend immunoagglutination test sensitivity while avoiding the prozone phenomenon, *J. Clin. Lig. Assay*, 1999, **22**, 410–412.
67 S. J. Gray, M. A. Sobanski, E. B. Kaczmarski, M. Guiver, W. J. Marsh, R. Borrow, R. A. Barnes and W. T. Coakley, Ultrasound-enhanced latex immunoagglutination and PCR as complementary methods for non-culture-based confirmation of meningococcal disease, *J. Clin. Microbiol.*, 1999, **37**, 1797–1801.
68 M. A. Sobanski, R. W. Ellis and J. G. M. Hastings, Rotavirus detection using ultrasound enhanced latex agglutination and turbidimetry, *J. Immunoassay*, 2000, **21**, 315–325.
69 M. A. Sobanski, R. A. Barnes, S. J. Gray, A. D. Carr, E. B. Kaczmarski, A. O'Rourke, K. Murphy, M. Cafferkey, R. W. Ellis, K. Pidcock, P. Hawtin and W. T. Coakley, Measurement of serum antigen concentration by ultrasound-enhanced immunoassay and correlation with clinical outcome in meningococcal disease, *Eur. J. Microbiol. Infect. Dis.*, 2000, **19**, 260–266.
70 M. A. Sobanski, J. Stephens, G. A. Biagini and W. T. Coakley, Detection of adenovirus and rotavirus antigens by an immuno-gold lateral flow test and ultrasound-enhanced latex agglutination assay, *J. Med. Microbiol.*, 2001, **50**, 203.
71 M. A. Sobanski, R. Vince, G. A. Biagini, C. Cousins, M. Guiver, S. J. Gray, E. B. Kaczmarski and W. T. Coakley, Ultrasound enhanced detection of individual meningococcal serogroups by latex immunoassay, *J. Clin. Pathol.*, 2002, **55**, 37–40.
72 R. J. Porritt, J. L. Mercer and R. Munro, Ultrasound-enhanced latex immunoagglutination test (USELAT) for detection of capsular polysaccharide antigen of Neisseria meningitidis from CSF plasma, *Pathology*, 2003, **35**, 61–64.
73 N. E. Thomas and W. T. Coakley, Measurement of antigen concentration by an ultrasound-enhanced latex immunoagglutination assay, *Ultrasound Med. Biol.*, 1996, **22**, 1277–1284.
74 S. Bhaskar, J. N. Banavaliker, K. Bhardwaj and U. Upadhyay, A novel ultrasound-enhanced latex agglutination test for the detection of antibodies against Mycobacterium tuberculosis in serum, *J. Immunol. Methods*, 2002, **262**, 181–186.
75 W. T. Coakley, J. J. Hawkes, M. A. Sobanski, C. M. Cousins and J. Spengler, Analytical scale ultrasonic standing wave manipulation of cells and microparticles, *Ultrasonics*, 2000, **38**, 638–641.
76 N. E. Thomas, M. E. Sobanski and W. T. Coakley, Ultrasonic enhancement of coated particle agglutination immunoassays: Influence of particle density and compressibility, *Ultrasound Med. Biol.*, 1999, **25**, 443–450.
77 J. Y. Yoon, K. H. Kim, S. W. Choi, J. H. Kim and W. S. Kim, Effects of surface characteristics on non-specific agglutination in latex immunoagglutination antibody assay, *Colloids Surf., B*, 2003, **27**, 3–9.
78 M. A. Sobanski, C. R. Tucker, N. E. Thomas and W. T. Coakley, Sub-micron particle manipulation in an ultrasonic standing wave: Applications in detection of clinically important biomolecules, *Bioseparation*, 2001, **9**, 351–357.
79 M. A. Sobanski, S. J. Gray, M. Cafferkey, R. W. Ellis, R. A. Barnes and W. T. Coakley, Meningitis antigen detection: interpretation of agglutination by ultrasound-enhanced latex immunoassay, *Br. J. Biomed. Sci.*, 1999, **56**, 239–246.
80 J. Frengen, K. Nustad, R. Schmid and T. Lindmo, A sequential binding assay with a working range extending beyond seven orders of magnitude, *J. Immunol. Methods*, 1995, **178**, 131–140.
81 Z. Rosenzweig and E. S. Yeung, Laser-based particle-counting microimmunoassay for the analysis of single human erythrocytes, *Anal. Chem.*, 1994, **66**, 1771–1776.
82 H. Nilsson, M. Wiklund, T. Johansson, H. M. Hertz and S. Nilsson, Microparticles for selective protein determination in capillary electrophoresis, *Electrophoresis*, 2001, **22**, 2384–2390.
83 I. V. Surovtsev, M. A. Yurkin, A. N. Shvalov, V. M. Nekrasov, G. F. Sivolobov, A. A. Grazhdantseva, V. P. Maltsev and A. V. Chernyshev, Kinetics of the initial stage of immunoagglutionation studied with the scanning flow cytometer, *Colloids Surf., B*, 2003, **32**, 245–255.
84 E. F. Ullman, H. Kirakossian, S. Singh, Z. P. Wu, B. R. Irvin, J. S. Pease, A. C. Switchenko, J. D. Irvine, A. Dafforn and C. N. Skold, et al., Luminescent oxygen channeling immunoassay: measurement of particle binding kinetics by chemiluminescence, *Proc. Natl. Acad. Sci. U. S. A.*, 1994, **91**, 5426–5430.
85 M. Wiklund, P. Spegel, S. Nilsson and H. M. Hertz, Ultrasonic-trap-enhanced selectivity in capillary electrophoresis, *Ultrasonics*, 2003, **41**, 329–333.
86 M. K. Araz, C. H. Lee and A. Lal, Ultrasonic separation in microfluidic capillaries, in *Proc. IEEE Ultrason. Symp.*, 2003, 1066–1069.
87 M. K. Araz and A. Lal, Ultrasonic chromatography in silicon-based microfluidic system, in *Proc. 9th International Conference on Miniaturized Systems for Chemistry and Life Sciences*, 2005, pp. 349–351.
88 T. Hatano, T. Kaneta and T. Imasaka, Application of optical chromatography to immunoassay, *Anal. Chem.*, 1997, **69**, 2711–2715.
89 P. K. Horan and L. L. Wheeless, Quantitative single cell analysis and sorting, *Science*, 1977, **198**, 149–157.
90 P. Hänninen, A. Soini, N. Meltola, J. Soini, J. Soukka and E. Soini, A new microvolume technique for bioaffinity assays using two-photon excitation, *Nat. Biotechnol.*, 2000, **18**, 548–550.
91 E. E. Swartzman, S. J. Miraglia, J. Mellentin-Michelotti, L. Evangelista and P. M. Yuan, A homogeneous and multiplexed immunoassay for high-throughput screening using fluorometric microvolume assay technology, *Anal. Biochem.*, 1999, **271**, 143–151.
92 H. E. Hart and E. B. Greenwald, Scintillation proximity assay (SPA): a new method of immunoassay. Direct and inhibition mode detection with human albumin and rabbit antihuman albumin, *Mol. Immunol.*, 1979, **16**, 265–267.
93 G. F. Blackburn, H. P. Shah, J. H. Kenten, J. Leland, R. A. Kamin, J. Link, J. Peterman, M. J. Powell, A. Shah and D. B. Talley, Electrochemiluminescence detection for development of immunoassays and DNA probe assays for clinical diagnostics, *Clin. Chem.*, 1991, **37**, 1534–1539.
94 R. P. Ekins, Multi-analyte immunoassay, *J. Pharm. Biomed. Anal.*, 1989, **7**, 155–168.
95 R. Ekins and F. Chu, Multianalyte microspot immunoassay. The microanalytical 'compact disk' of the future, *Ann. Biol. Clin.*, 1992, **50**, 337–353.
96 C. Zhou, P. Pivarnik, A. G. Rand and S. V. Lethcher, Acoustic standing-wave enhancement of a fiber-optic Salmonella biosensor, *Biosens. Bioelectron.*, 1998, **13**, 495–500.
97 S. P. Martin, R. J. Townsend, L. A. Kuznetsova, K. A. J. Borthwick, M. Hill, M. B. McDonnell and W. T. Coakley, Spore and micro-particle capture on an immunosensor surface in an ultrasound standing wave system, *Biosens. Bioelectron.*, 2005, **21**, 758–767.
98 L. A. Kuznetsova, S. P. Martin and W. T. Coakley, Sub-micron particle behavoiur and capture at an immuno-sensor surface in an ultrasonic standing wave, *Biosens. Bioelectron.*, 2005, **21**, 940–948.
99 M. I. Song, K. Iwata, M. Yamada, K. Yokoyama, T. Takeuchi, E. Tamiya and I. Karube, Multisample analysis using an array of microreactors for an alternating-current field-enhanced latex immunoassay, *Anal. Chem.*, 1994, **66**, 778–781.
100 J. Auerswald, D. Widmer, N. F. de Rooij, T. Stöckli, A. Sigrist, T. Staubli and H. F. Knapp, Fast microarray functionalization with probe beads for lab-on-chip affinity assay, in *Proc. 9th International Conference on Miniaturized Systems for Chemistry and Life Sciences*, ed. K. F. Jensen, J. Han, D. J. Harrison and J. Voldman, Boston, MA, 2005, pp. 1054–1056.

101 Y.-C. Tseng, K. D. Burman, J. R. Baker and L. Wartofsky, A rapid, sensitive enzyme-linked immunoassay for Human Thyrotropin, *Clin. Chem.*, 1985, **31**, 1131–1134.
102 Å. K. Rasmussen, L. Hilsted, H. Perrild, E. Christiansen, K. Siersbaek-Nielsen and U. Feldt-Rasmussen, Discrepancies between thyrotropin (TSH) measurement by four sensitive immunometric assays, *Clin. Chim. Acta*, 1997, **259**, 117–128.
103 J. O. Koskinen, N. J. Meltola, E. Soini and A. E. Soini, A lab-on-a-chip compatible bioaffinity assay method for human α-fetoprotein, *Lab Chip*, 2005, **5**, 1408–1411.
104 J. O. Koskinen, J. Vaarno, N. J. Meltola, J. T. Soini, P. E. Hänninen, J. Luotola, M. E. Waris and A. E. Soini, Fluorescent nanoparticles as labels for immunometric assay of C-reactive protein using two-photon excitation assay technology, *Anal. Biochem.*, 2004, **328**, 210–218.
105 J. O. Koskinen, J. Vaaro, R. Vainionpaa, N. J. Meltola and A. E. Soini, A novel separation-free assay technique for serum antibodies using antibody bridging assay principle and two-photon excitation fluorometry, *J. Immunol. Methods*, 2006, **309**, 11–24.
106 J. M. Nam, C. S. Thaxton and C. A. Mirkin, Nanoparticle-based bio-bar codes for the ultrasensitive detection of proteins, *Science*, 2003, **301**, 1884–1886.
107 T. Soukka, J. Paukkunen, H. Härmä, S. Lönnberg, H. Lindroos and T. Lövgren, Supersensitive time-resolved immunofluorometric assay of free prostate-specific antigen with nanoparticle label technology, *Clin. Chem.*, 2001, **47**, 1269–1278.